Fermi National Accelerator Laboratory

FERMILAB-Conf-95/291-E
D0

Observation of the Top Quark

J. Bantly
For the D0 Collaboration

Fermi National Accelerator Laboratory
P.O. Box 500, Batavia, Illinois 60510

Brown University
Providence, Rhode Island 02912

October 1995

Published Proceedings of the *10th Topical Workshop on Proton-Antiproton Collider Physics,* Fermi National Accelerator Laboratory, Batavia, Illinois, May 9-13, 1995

Disclaimer

FERMILAB-Conf-95/291-E
DØ

Observation of the Top Quark *

Jeffrey Bantly

Brown University
Providence, RI 02912

for

The DØ Collaboration

Abstract

The DØ collaboration reports on a search for the Standard Model top quark in $p\bar{p}$ collisions at $\sqrt{s} = 1.8$ TeV at the Fermilab Tevatron, with an integrated luminosity of approximately 50 pb^{-1}. We have searched for $t\bar{t}$ production in the dilepton and single-lepton decay channels, with and without tagging of b quark jets. We observe 17 events with an expected background of 3.8 ± 0.6 events. The probability for an upward fluctuation of the background to produce the observed signal is 2×10^{-6} (equivalent to 4.6 standard deviations). The kinematic properties of the excess events are consistent with top quark decay. We conclude that we have observed the top quark and measure its mass to be 199^{+19}_{-21} (stat.) ± 22 (syst.) GeV/c^2 [1)] and its production cross section to be 6.4 ± 2.2 pb. Other decay channels are under study such as the $t\bar{t}$ to all-jets channel which might yield additional information about the top quark.

*presented at the 10th Topical Workshop on Proton-Antiproton Collider Physics (PbarP 95), Fermi National Accelerator Laboratory, Batavia, IL, May 9-13, 1995.

1 Introduction

The Standard Model requires that the b quark have a weak isospin partner, the hitherto unobserved top quark. The search for the top quark and the measurement of its properties are important tests of the Standard Model. Certain Standard Model parameters, including m_W, m_Z, $\sin^2\theta_W$, and Z boson decay asymmetries depend on the top quark mass, and to a lesser extent on the Higgs boson mass, through radiative corrections involving top quark loops. Precision measurements of these parameters permit an indirect measurement of the top quark mass which can be compared to that obtained by direct measurement. These precision measurements currently suggest a top quark mass in the range 150–210 GeV/c^2 [2].

The most sensitive searches for the Standard Model top quark have been carried out at the Fermilab Tevatron by the CDF and DØ experiments. Recent results from these experiments, based on data from the 1992–1993 Tevatron run (run Ia), include a lower limit on m_t of 131 GeV/c^2 by DØ [3], a 2.8σ positive result by CDF [4], and a 1.9σ result by DØ [5].

In this article, we assume that the top quark is pair-produced and decays 100% of the time into a W boson and a b quark. The search is divided into seven distinct channels depending on how the two W bosons decay, and on whether or not a soft muon from a b or c quark semileptonic decay is observed. The so-called dilepton channels occur when both W bosons decay leptonically ($e\mu$ + jets, ee + jets, and $\mu\mu$ + jets). The single-lepton channels occur when just one W boson decays leptonically (e + jets and μ + jets). The single-lepton channels are subdivided into b-tagged and untagged channels according to whether or not a muon is observed consistent with $b \to \mu + X$. The muon-tagged channels are denoted e + jets/μ and μ + jets/μ. The data set for this analysis includes data from run Ia and run Ib with an integrated luminosity of about 50pb^{-1}, with slight differences among the seven channels. The new results from CDF [6] and DØ [7] based on new data from the ongoing 1994–1995 Tevatron run (run Ib) have increased the significance of the top quark signal to $> 4\sigma$.

2 Particle Detection

The DØ detector and data collection systems are described in Ref. [8].

Muons are detected and momentum-analyzed using an iron toroid spectrometer located outside of a uranium-liquid argon calorimeter and a non-magnetic central tracking system inside the calorimeter. Muons are identified by their ability to penetrate the calorimeter and the spectrometer magnet yoke. Two distinct types of muons are defined. "High-p_T" muons, which are predominantly from gauge boson decay, are required to be isolated from jet axes by distance $\Delta\mathcal{R} > 0.5$ in η-ϕ space (η = pseudorapidity = $\tanh^{-1}(\cos\theta)$; θ, ϕ = polar, azimuthal angle), and to have transverse momentum $p_T > 12$ GeV/c. "Soft" muons, which are primarily from b, c or π/K decay, are required to be within distance $\Delta\mathcal{R} < 0.5$ of any jet axis. The minimum p_T for soft muons is 4 GeV/c. The maximum η for both kinds of muons is 1.7 for run Ia data and 1.0 for run Ib data. The maximum muon η is determined by the edge of the wide angle muon spectrometer. The η restriction is tightened for some run Ib data due to forward muon chamber aging.

Electrons are identified by their longitudinal and transverse shower profile in the calorimeter

and are required to have a matching track in the central tracking chambers. The background from photon conversions is suppressed by an ionization (dE/dx) criterion on the chamber track. A transition radiation detector is used to confirm the identity of electrons for $|\eta| < 1$. Electrons are required to have $|\eta| < 2.5$ and transverse energy $E_T > 15$ GeV.

Jets are reconstructed using a cone algorithm of radius $\mathcal{R} = 0.5$.

The presence of neutrinos in the final state is inferred from missing transverse energy ($\not\!\!E_T$). The calorimeter-only $\not\!\!E_T$ ($\not\!\!E_T^{\rm cal}$) is determined from energy deposition in the calorimeter for $|\eta| < 4.5$. The total $\not\!\!E_T$ is determined by correcting $\not\!\!E_T^{\rm cal}$ for the measured p_T of detected muons.

3 The Counting Experiment

The event selection for this analysis is chosen to give maximum expected significance for top quark masses of 180–200 GeV/c^2, using the ISAJET event generator [9] to model the top quark signal (assuming the Standard Model top quark pair production cross section of Ref. [10]), and using our standard background estimates as described below. In this analysis, we achieve a signal-to-background ratio of 1:1 for a top quark mass of 200 GeV/c^2. This is a better signal-to-background ratio, but with smaller acceptance, than our previously published analyses [3, 5]. The improved rejection arises primarily by requiring events to have a larger total transverse energy by means of a cut on a quantity we call H_T. H_T is defined as the scalar sum of the E_T's of the jets (for the single-lepton and $\mu\mu$ + jets channels), or the scalar sum of the E_T's of the leading electron and the jets (for the $e\mu$ + jets and ee + jets channels). In addition to our "standard" event selection, we define a "loose" event selection which does not include an H_T cut. We do this as a consistency check, and to provide a less biased event sample for the top quark mass analysis.

The signature for the dilepton channels is defined as two isolated leptons, two or more jets, and large $\not\!\!E_T$. The signature for the single-lepton channels is defined as one isolated lepton, large $\not\!\!E_T$, and three or more jets (with muon tag) or four or more jets (without tag). The single-lepton signature includes either a soft muon tag or a "topological tag" based on H_T and the aplanarity of the jets $\mathcal{A}$. The aplanarity is proportional to the smallest eigenvalue of the momentum tensor of the jets in the laboratory [11] and ranges from 0–0.5. "Double-tagged" events are counted only once, as part of the muon tagged channels. A summary of the kinematic cuts can be found in Table 1.

Additional special cuts are used in the ee + jets, $\mu\mu$ + jets, and μ + jets/μ channels to remove background from Z + jets. To remove $Z \rightarrow ee$ background in ee + jets, we require that $|m_{ee} - m_Z| > 12$ GeV/c^2 or $\not\!\!E_T^{\rm cal} > 40$ GeV. Because of DØ's coarse muon momentum resolution, which is limited by multiple scattering to about 20%, a dimuon invariant mass cut does not effectively remove background from $Z \rightarrow \mu\mu$ with reasonable efficiency. To remove this background, we require that the event as a whole is inconsistent with the Z + jets hypothesis based on a global kinematic fit (see Fig. 1). Note that although the $\mu\mu$ + jets channel does not explicity include a $\not\!\!E_T$ cut, it is hard for low-$\not\!\!E_T$ events to pass the kinematic fit. The loose event selection cuts differ from those listed in Table 1 by the removal of the H_T requirement and by the relaxation of the aplanarity requirement for e + jets and μ + jets from $\mathcal{A} > 0.05$ to

Table 1: Minimum kinematic requirements for the standard event selection (energy in GeV).

	High-p_T Leptons		Jets		Missing E_T		Muon Tag	Topological	
Channel	$E_T(e)$	$p_T(\mu)$	$N_{\rm jet}$	E_T(jet)	$\not\!\!E_T^{\rm cal}$	$\not\!\!E_T$	$p_T(\mu)$	H_T	$\mathcal{A}$
$e\mu$ + jets	15	12	2	15	20	10	-	120	-
ee + jets	20		2	15	25	-	-	120	-
$\mu\mu$ + jets		15	2	15	-	-	-	100	-
e + jets	20		4	15	25	-	-	200	0.05
μ + jets		15	4	15	20	20	-	200	0.05
e + jets/μ	20		3	20	20	-	4	140	-
μ + jets/μ		15	3	20	20	20	4	140	-

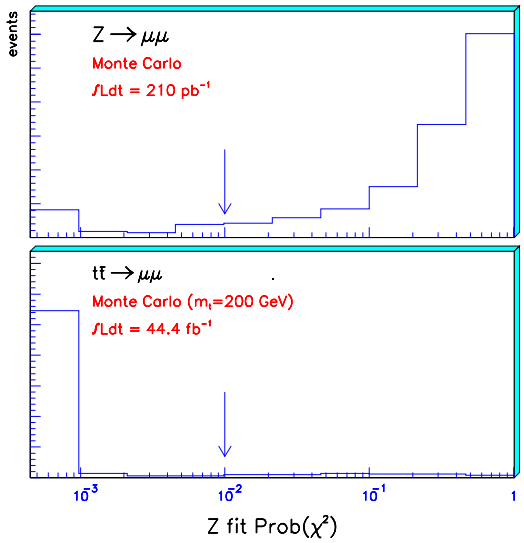

Figure 1: Chisquare probability distributions obtained from a global kinematic fit to the $Z(\rightarrow \mu\mu)$ + jets hypothesis for (a) $Z \rightarrow \mu\mu$ + jets Monte Carlo and (b) $t\bar{t} \rightarrow \mu\mu$ + jets Monte Carlo. We require $P(\chi^2) < 0.01$.

$\mathcal{A} > 0.03$.

H_T is a powerful discriminator between background and high-mass top quark production. Figure 2 shows a comparison of the shapes of the H_T distributions expected from background and 200 GeV/c^2 top quarks in the channels (a) $e\mu$ + jets and (b) untagged single-lepton + jets. We have tested our understanding of background H_T distributions by comparing data and calculated background in background-dominated channels such as electron + $\not\!\!E_T$ + two jets and electron + $\not\!\!E_T$ + three jets (see Fig. 3). The observed H_T distribution agrees with the background calculation, which includes contributions from both W + jets as calculated by the VECBOS Monte Carlo [12] and QCD multijet events.

The acceptance for $t\bar{t}$ events is calculated using the ISAJET event generator and a detector simulation based on the GEANT program [13]. As a check, the acceptance is also calculated using the HERWIG event generator [14]. The difference between ISAJET and HERWIG is included

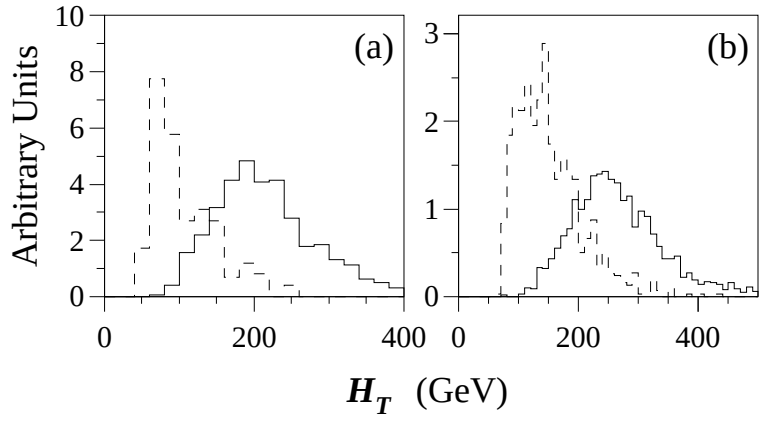

Figure 2: Shape of H_T distributions expected for the principal backgrounds (dashed line) and 200 GeV/c^2 top quarks (solid line) for (a) $e\mu$ + jets and (b) untagged single-lepton + jets.

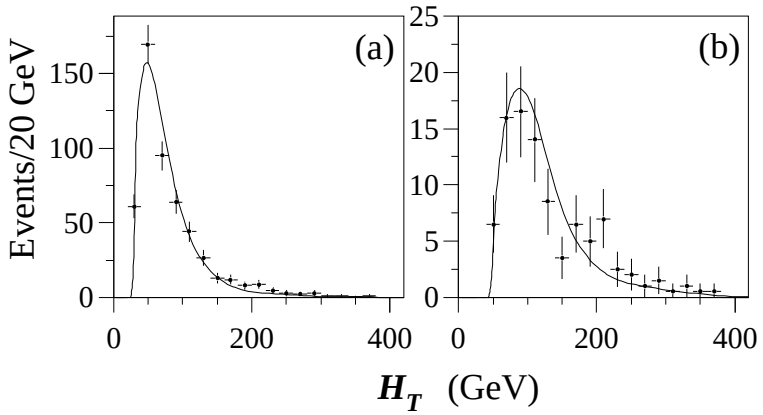

Figure 3: Observed H_T distributions (points) compared to the distributions expected from background (curve) for $\not\!\!E_T > 25$ GeV and (a) $e + \geq 2$ jets and (b) $e + \geq 3$ jets.

in the systematic error.

Physics backgrounds (those having the same final state particles as the signal) are estimated using Monte Carlo simulation, or a combination of Monte Carlo and data. The instrumental background from jets misidentified as electrons is estimated entirely from data using the measured jet misidentification probability (typically 2×10^{-4}). Other backgrounds for muons (*e.g.* hadronic punchthrough and cosmic rays) are negligible for the signatures in question.

For the dilepton channels, the principle backgrounds are from Z and continuum Drell-Yan production ($Z, \gamma^* \rightarrow ee, \mu\mu$, and $\tau\tau$), vector boson pairs (WW, WZ), heavy flavor ($b\bar{b}$ and $c\bar{c}$) production, and backgrounds with jets misidentified as leptons.

For the untagged single-lepton channels, the principle backgrounds are from W + jets, Z + jets, and QCD multijet production with a jet misidentified as a lepton. The W + jets background is estimated using jet-scaling. In this method, we extrapolate the W + jets cross section from one and two jets, to four or more jets assuming an exponential dependence on

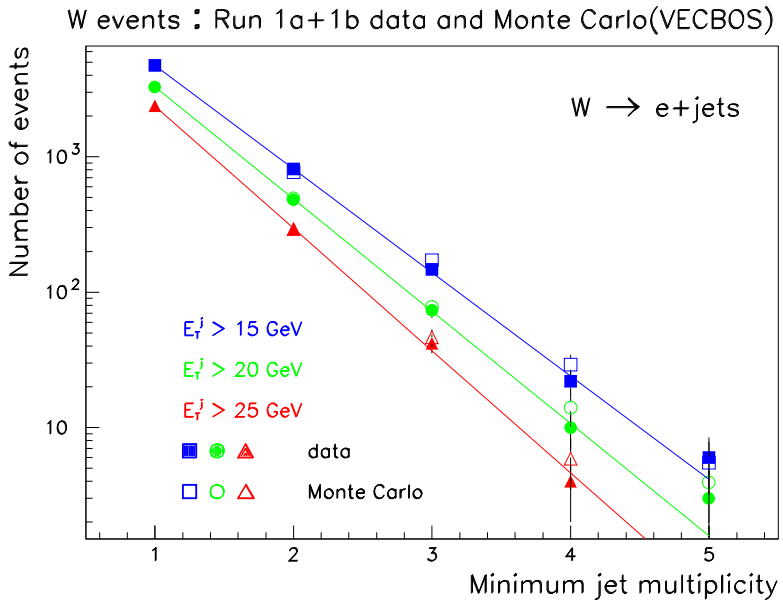

Figure 4: Inclusive jet multiplicity spectrum for $W \rightarrow e +$ jets events for several jet energy thresholds. Data are shown by the solid symbols; Monte Carlo predictions are shown by the open symbols.

the number of jets, as predicted by QCD [12], and as observed experimentally (see Fig. 4). The efficiency of the topological cuts for W + 4 jets is calculated using the VECBOS Monte Carlo program [12]. The QCD multijet background is determined independently from data using the measured jet fake probability. The Z + jets background is estimated by Monte Carlo calculation.

For the tagged single-lepton channels, the observed jet multiplicity spectrum of untagged background events is convoluted with the measured tagging rate per jet to determine the total background. The tagging rate is observed to be a function of the number of jets in the event and the E_T of the jets and is the same within error for both multijet and W +jets events. As a cross check, tagging-rate predictions are made for dijet, multijet, and gamma+jet samples and found to agree with the data.

From all seven channels, we observe 17 events with an expected background of 3.8 ± 0.6 events (see Table 2). Our measured cross section as a function of the top quark mass hypothesis is shown in Fig. 6. Assuming a top quark mass of 200 GeV/c^2, the production cross section is 6.3 ± 2.2 pb. The error in the cross section includes an overall 12% uncertainty in the luminosity. The probability of an upward fluctuation of the background to 17 or more events is 2×10^{-6}, which corresponds to 4.6 standard deviations for a Gaussian probability distribution. The excess is distributed across all of the channels in a manner consistent with Standard Model top quark decay branching ratios (see Tables 3–5). We conclude that we have observed the top quark. Supporting results for the top quark observation include two-jet vs. three-jet mass distributions and the determination of the top quark mass presented elsewhere in these proceedings [1].

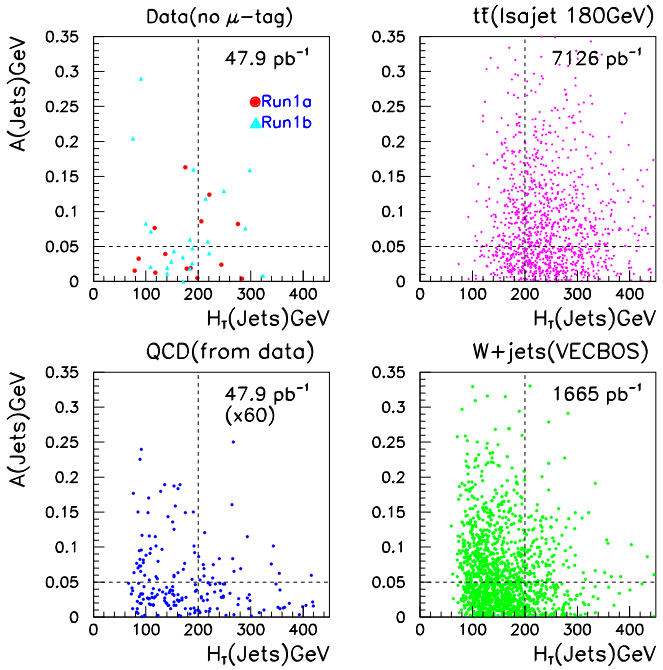

Figure 5: $\mathcal{A}$ *vs.* H_T for single-lepton events for data (13.5 pb^{-1}), 180 GeV/c^2 top ISAJET Monte Carlo (7126 pb^{-1}), multijet background from data (effective luminosity = 60 $\times$ data luminosity), and background from W + 4 jet VECBOS Monte Carlo (1665 pb^{-1}).

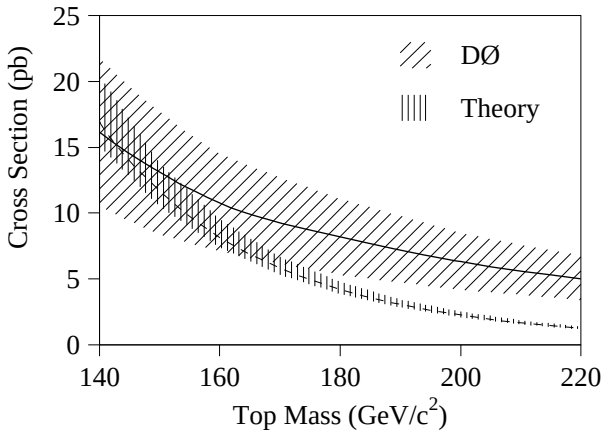

Figure 6: DØ measured $t\bar{t}$ production cross section (solid line with one standard deviation error band) as a function of assumed top quark mass. Also shown is the theoretical cross section curve (dashed line) [10].

4 Additional Channels Under Study - $t\bar{t} \rightarrow$ all jets

In the Standard Model, the dominant decay channel for top quarks is a b quark and a W boson, with the W boson decaying into a quark-antiquark pair. Events with t and $\bar{t}$ quarks present can have both W bosons decaying to quarks. This is referred to as the "all-jets" channel and nominally accounts for 44% of the $t\bar{t}$ cross section.

The signature for $t\bar{t}$ production in the all-jets channel is six (or more) high momentum

Table 2: Counting experiment summary for all channels.

	Standard Selection	Loose Selection
Dileptons	3	4
Lepton + Jets (Topological)	8	23
Lepton + Jets (Muon tag)	6	6
All channels	17	33
Background	3.8 ± 0.6	20.6 ± 3.2
Probability	2×10^{-6} (4.6σ)	0.023 (2.0σ)
$\sigma_{t\bar{t}}$ $(m_t = 200$ GeV/c$^2)$	6.3 ± 2.2 pb	4.5 ± 2.5 pb

Table 3: Counting experiment summary for the dilepton channels.

	Standard Selection	Loose Selection
Data	3	4
Background	0.65 ± 0.15	2.66 ± 0.40
Probability	0.03 (1.9σ)	0.28 (0.6σ)
$\sigma_{t\bar{t}}$ $(m_t = 200$ GeV/c$^2)$	7.5 ± 5.7 pb	4.4 ± 6.8 pb

jets, with kinematic properties consistent with a $t\bar{t}$ decay hypothesis. The background for this signature consists of events from other processes that can also produce six or more jets, with similar kinematic properties. The search for the top quark in the all-jets channel begins with the imposition of preliminary selection criteria at the trigger stage and in the offline analysis. These criteria include 6 or more jets > 10 GeV with $|\eta| < 2$, no isolated electron ($E_T^e < 20$ GeV) or muon ($p_T^\mu < 15$ GeV/c), and $H_T > 150$ GeV using only the jets with $E_T > 15$ GeV with $|\eta| < 2$. These criteria are not very restrictive, and the observed cross section is more than one thousand times larger than the expected signal. The principal challenge in this search is to develop a set of selection criteria that can significantly improve the signal to background ratio and provide an estimate of the remaining background.

In addition to the initial selection, we use four additional kinematic parameters: the scalar sum of jet E_T excluding the two leading jets (H_T^{3j}), the aplanarity ($\mathcal{A}$), the centrality ($\mathcal{C}$) of the event given by the ratio of H_T to H_E, where H_E is the sum of jet energies, and the averaged

Table 4: Counting experiment summary for the topological single-lepton channels.

	Standard Selection	Loose Selection
Data	8	23
Background	1.9 ± 0.5	15.7 ± 3.1
Probability	0.002 (2.9σ)	0.09 (1.3σ)
$\sigma_{t\bar{t}}$ $(m_t = 200$ GeV/c$^2)$	4.9 ± 2.5 pb	4.0 ± 3.2 pb

Table 5: Counting experiment summary for the muon-tagged single-lepton channels.

	Standard Selection	Loose Selection
Data	6	6
Background	1.2 ± 0.2	2.2 ± 0.3
Probability	0.002 (2.9σ)	0.03 (1.9σ)
$\sigma_{t\bar{t}}$ (m_t = 200 GeV/c^2)	8.9 ± 4.8 pb	6.3 ± 4.2 pb

number of jets (N_j^{Ave}). The averaged number of jets is the number of jets averaged over a range of E_T thresholds, weighted by the E_T threshold.

After applying criteria based on the above parameters, we require a soft muon to tag the b-jets. Because every $t\bar{t}$ event contains two high-E_T b-quark jets, this requirement enriches the $t\bar{t}$ component of the sample, roughly by an order of magnitude.

Due to a lack of reliable Monte Carlo sample for background processes, the entire Run Ia data sample is used to model background properties, and the search for signal is concentrated only on Run Ib data. The sacrifice of a large portion of the data sample, containing a quarter of the available luminosity, ensures that the criteria are derived from an event sample that is statistically independent of the data used in the search.

4.1 Four Kinematic Parameters

We will differentiate between $t\bar{t}$ signal and background using the variables aplanarity ($\mathcal{A}$), H_T with the leading two jets excluded (H_T^{3j}), centrality ($\mathcal{C}$), and the average jet count parameter N_j^{Ave}.

Distributions in these parameters are shown in Figs. 7, 8, 9, and 10. In each figure, the data from Run I (a+b) are shown with the solid points. The results for the $t\bar{t}$ Monte Carlo m_t=200 GeV/c^2 are shown with the dashed points and the $t\bar{t}$ Monte Carlo m_t=160 GeV/c^2 are shown with the dotted points. The distributions are normalized to cross section. The top signal is generally distributed towards the higher values for H_T H_T^{3j}, $\mathcal{C}$, and N_j^{Ave}yet the background dominates even in the tails. The definitions of our parameters are reviewed below.

Aplanarity is an effective background discriminator in the region of $\mathcal{A} < 0.15$ as shown in Fig. 7, but the signal to background ratio (S/B) changes slowly with $\mathcal{A}$. $\mathcal{A}$ is relatively insensitive to the mass of the top quark, and the distributions for m_t=160 and 200 GeV/c^2 have nearly the same shape.

A variant of H_T, one in which the two leading E_T jets are not included, is defined as:

$$H_T^{3j} = \sum_{nj=3}^{N} |E_T| \, .$$

H_T^{3j} can be used to discriminate against background processes in which the event topology is dominated by two leading jets, a characteristic of QCD di-jet production in which additional jets are generated with lower E_T. H_T^{3j} depends strongly on the mass of the top quark, as can

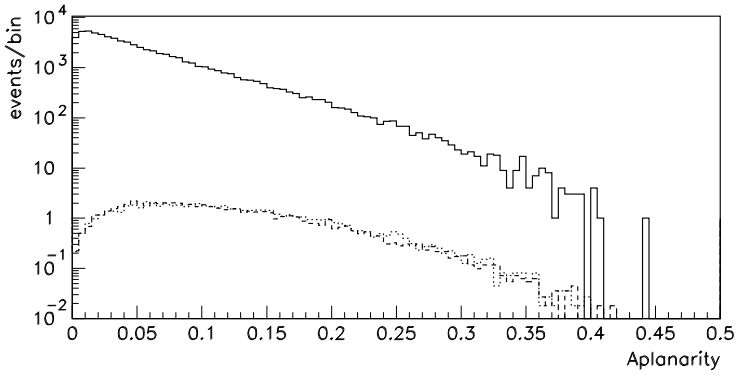

Figure 7: Distributions in aplanarity for data from Run I (solid points) and for ISAJET $t\bar{t}$ Monte Carlo for m_t=200 GeV/c^2 (dashed points) and m_t=160 GeV/c^2 (dotted points), normalized to cross section.

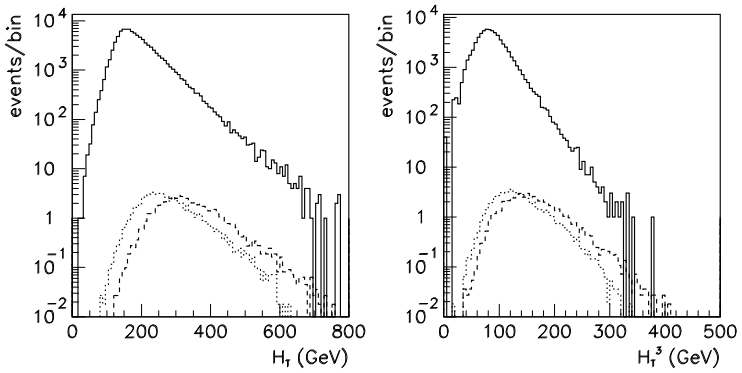

Figure 8: Distributions in H_T and H_T^{3j} for data from Run I (solid points) and for ISAJET $t\bar{t}$ Monte Carlo for m_t=200 GeV/c^2 (dashed points) and m_t=160 GeV/c^2 (dotted points), normalized to cross section.

be seen in Fig. 8, where in the region beyond $H_T^{3j} \approx 200$ GeV, the distribution for m_t=160 falls faster than m_t=200 GeV/c^2 . For H_T^{3j} thresholds near 300 GeV, the signal to background ratio approaches 1:3. We see that H_T^{3j} is clearly a better discriminator between signal and background than $\mathcal{A}$.

The centrality ($\mathcal{C}$) of an event is the ratio of transverse (H_T) to the sum of total jet energies. Decay products from $t\bar{t}$ tend to be emitted closer to $|\eta| = 0$ than jets from background processes. An event with all jets near η=0 will have $\mathcal{C} \simeq 1$, while events with forward jets will have $\mathcal{C}$ values as low as 0.4. In the region of $\mathcal{C} < 0.7$, centrality is a useful discriminator; beyond 0.7, signal and background have similar dependence on $\mathcal{C}$.

Finally, the average jet count parameter is defined as:

$$N_j^{Ave} = \frac{\int_{15}^{45} E_T^{thr} N(E_T^{thr}) dE_T^{thr}}{\int_{15}^{45} E_T^{thr} dE_T^{thr}},$$

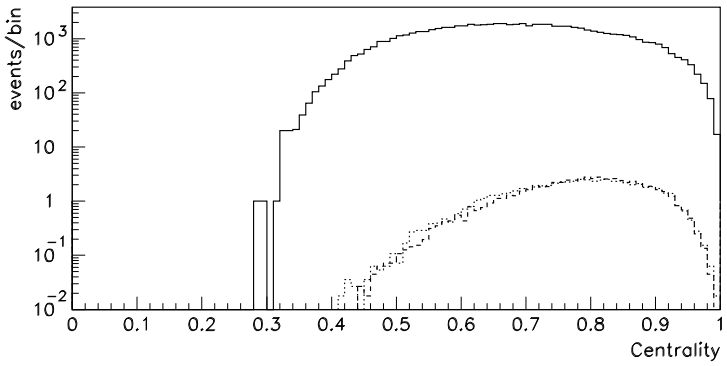

Figure 9: Distributions in centrality for data from Run I (solid points) and for ISAJET $t\bar{t}$ Monte Carlo for m_t=200 GeV/c^2 (dashed points) and m_t=160 GeV/c^2 (dotted points), normalized to cross section.

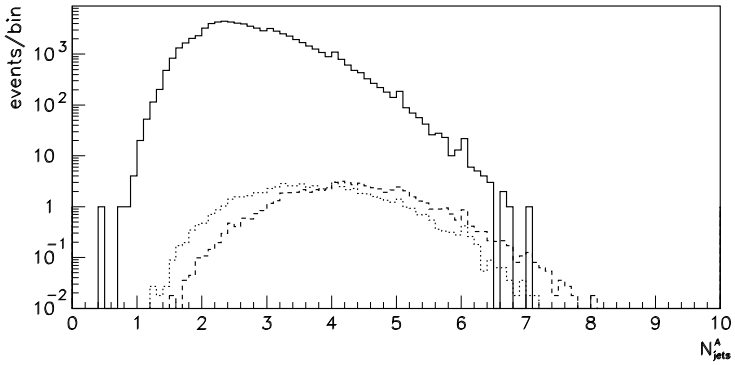

Figure 10: Distributions in average number of jets for data from Run I (solid points) and for ISAJET $t\bar{t}$ Monte Carlo for m_t=200 GeV/c^2 (dashed points) and m_t=160 GeV/c^2 (dotted points), normalized to cross section.

which is the number of jets averaged over a range of E_T thresholds (from 15 to 45 GeV) and weighted by the E_T threshold. The advantage of this parameter are that it is a continuous measure of jet multiplicity and that it has more sensitivity to jets of higher E_T than a jet count with some given threshold.

A grid search of variations in the four kinematic parameter selection cuts is used to determine optimal combinations of cuts for a given desired signal to background ratio and number of desired signal events remaining.

4.2 Muon-tagging of Jets

Muon-tagging in the all jets channel is done in the same way as the lepton+jets channel except the jets have a R=0.3 cone size. Muon tagging can achieve additional background rejection but

Selection criteria	$\mathcal{C}$	N_j^{Ave}	$\mathcal{A}$	H_T^{3j} (GeV)	N_{bkg} μ-tagged	$N_{t\bar{t}}$ μ-tagged
loose	0.658	3.64	0.055	135.3	41.4	8.7
medium	0.662	4.60	0.055	165.4	10.1	4.7
tight	0.700	5.10	0.100	188.0	1.5	1.9

Table 6: Threshold values for three sets of cuts with the expected numbers of background and signal events for Run Ib. The background prediction is made using data from Run Ia and the μ-tag rate from Run Ib.

Selection criteria	No. Run Ib events	$N_{t\bar{t}}$ (m_t=200 GeV/c^2)	N_{bkg} μ-tag	observed μ-tag	expected $t\bar{t}$ μ-tag
none	58327	104.1	1017.5	1053	22.1
loose	1459	48.2	40.8	50	10.4
medium	369	25.5	11.6	13	5.4
tight	66	9.8	2.3	4	2.3

Table 7: Comparison of number of μ-tagged events in Run Ib with expected background and $t\bar{t}$ signal. The number of $t\bar{t}$ events includes contributions from other top quark decay channels that pass the selection criteria.

the cost is a substantial loss of potential signal. This loss in efficiency is acceptable because μ-tagging provides a straightforward and reliable way to estimate the background expected in a data sample. The background tag rate is parameterized as a function of jet E_T, and this tag rate function is applied to the candidate sample of events to estimate the background.

4.3 A Sample of Preliminary Results from the All Jets channel

For three sets of selection cuts, listed in Table 6, the number of predicted signal (using Isajet 200 GeV $t\bar{t}$ Monte Carlo), the expected background, and the number of observed data events is shown in Table 7. These preliminary results show evidence for a small excess. With the tight selection cuts shown, a signal to background of nearly 1 to 1 is achieved. Future studies will hopefully improve the all jets channel results for inclusion in the calculated top cross section.

5 Conclusions

We have searched for top quark signals in seven channels in a data sample having an integrated luminosity of 50 pb^{-1}. We observe 17 candidate events with an expected background of 3.8 ± 0.6 events. The excess is statistically significant. The probability for the background to fluctuate up to 17 events is 2×10^{-6}, which corresponds to 4.6σ in the case of Gaussian errors. We measure the top quark mass to be 199^{+19}_{-21}(stat.) $\pm$ 22(syst.)GeV/c^2. Using the acceptance calculated at our central top quark mass, we measure the top quark pair production cross section to be

$\sigma_{t\bar{t}} = 6.4 \pm 2.2$ pb. Additional channels, such as $t\bar{t}$ to all jets, are being analyzed to broaden our understanding of top quark physics.

We thank the Fermilab Accelerator, Computing, and Research Divisions, and the support staffs at the collaborating institutions for their contributions to the success of this work. We also acknowledge the support of the U.S. Department of Energy, the U.S. National Science Foundation, the Commissariat à L'Energie Atomique in France, the Ministry for Atomic Energy and the Ministry of Science and Technology Policy in Russia, CNPq in Brazil, the Departments of Atomic Energy and Science and Education in India, Colciencias in Colombia, CONACyT in Mexico, the Ministry of Education, Research Foundation and KOSEF in Korea, and the A. P. Sloan Foundation.

References

[1] M. Strovink (DØ Collaboration), to be published in the proceedings of the 10th Topical Workshop on Proton-Antiproton Collider Physics (PbarP 95), Fermi National Accelerator Laboratory, Batavia, IL, May 9-13, 1995. See also FERMILAB-Conf-95/189-E.

[2] D. Schaile, CERN-PPE/94-162, presented at 27th International Conference on High Energy Physics, Glasgow, July 1994 (unpublished).

[3] S. Abachi *et al.*, DØ Collaboration, Phys. Rev. Lett. **72**, 2138 (1994).

[4] F. Abe *et al.*, CDF Collaboration, Phys. Rev. D **50**, 2966 (1994); Phys. Rev. Lett. **73**, 225 (1994).

[5] S. Abachi *et al.*, DØ Collaboration, Phys. Rev. Lett. **74**, 2422 (1995).

[6] F. Abe *et al.*, CDF Collaboration, Phys. Rev. Lett. **74**, 2626 (1995).

[7] S. Abachi *et al.*, DØ Collaboration, Phys. Rev. Lett. **74**, 2632 (1995).

[8] S. Abachi *et al.*, DØ Collaboration, Nucl. Instrum. Methods **A338**, 185 (1994).

[9] F. Paige and S. Protopopescu, BNL Report no. BNL38034, 1986 (unpublished), release v6.49.

[10] E. Laenen, J. Smith, and W. van Neerven, Phys. Lett. **321B**, 254 (1994).

[11] V. D. Barger and R. J. N. Phillips, *Collider Physics*, Addison-Wesley Publishing Co. (1987), p. 281.

[12] F. A. Berends, H. Kuijf, B. Tausk, and W. T. Giele, Nucl. Phys. B357, 32 (1991).

[13] F. Carminati *et al.*, "GEANT Users Guide," CERN Program Library, 1991 (unpublished).

[14] G. Marchesini *et al.*, Comput. Phys. Commun. **67**, 465, (1992).